Article

Probing dynamic conformations of the high molecular weight #B-crystallin heat shock protein ensemble by NMR spectroscopy

Andrew James Baldwin, Patrick Walsh, D. Flemming Hansen, Gillian
Ruth Hilton, Justin LP Benesch, Simon Sharpe, and Lewis Edward Kay

Just Accepted

1
2
3
4
5
6
7
8
9
10
11
12
13
14
15
16
17
18
19
20
21
22
23
24
25
26
27
28
29
30
31
32
33
34
35
36
37
38
39
40
41
42
43
44
45
46
47
48
49
50
51
52
53
54
55
56
57
58
59
60

Probing dynamic conformations of the high molecular weight αB-crystallin heat shock protein ensemble by NMR spectroscopy

Andrew J. Baldwin[1,2]*, Patrick Walsh[2,3], D. Flemming Hansen[1]†, Gillian R. Hilton[4], Justin L.P. Benesch[4], Simon Sharpe[2,3], Lewis E. Kay[1,2,3]*

[1]Departments of Molecular Genetics and Chemistry, The University of Toronto, Toronto, Ontario, M5S 1A8, Canada

[2]Department of Biochemistry, The University of Toronto, Toronto, Ontario, M5S 1A8, Canada

[3]Hospital for Sick Children, Program in Molecular Structure, 555 University Avenue, Toronto, Ontario, M5G 1X8, Canada

[4]Department of Chemistry, Physical and Theoretical Chemistry Laboratory, University of Oxford, South Parks Road, Oxford, Oxfordshire, OX1 3QZ, U.K.

†Present Address: Institute of Structural and Molecular Biology, University College London, London, United Kingdom, WC1E 6BT

ABSTRACT

Solution- and solid-state NMR spectroscopy are highly complementary techniques for studying supra-molecular structure. Here they are employed for investigating the molecular chaperone αB-crystallin, a polydisperse ensemble of between $10 - 40$ identical subunits with an average molecular mass of approximately 600 kDa. An IxI motif in the C-terminal region of each of the subunits is thought to play a critical role in regulating the size distribution of oligomers and in controlling the kinetics of subunit exchange between them. Previously published solid-state NMR and X-ray results are consistent with a bound IxI conformation while solution NMR studies provide strong support for a highly dynamic state. Here we demonstrate through FROSTY MAS NMR that both populations are present at low temperatures ($< 0^{o}$C), while at higher temperatures only the mobile state is observed. Solution NMR relaxation dispersion experiments performed under physiologically relevant conditions, establish that the motif interchanges between flexible (highly populated) and bound (sparsely populated) states. This work emphasizes the importance of using multiple methods in studies of supra-molecules, especially for highly dynamic ensembles where sample conditions can potentially affect the conformational properties observed.

Introduction

The native states of proteins are in many cases inherently unstable[1] and the assistance of 'molecular chaperones' is required to ensure that these important biomolecules attain and maintain their functional forms[2,3]. The molecular chaperone αB-crystallin is a human small heat shock protein (sHSP) that plays an important role in proteostasis *in vivo*[4,5] and it can prevent amyloid fibril formation *in vitro*[6]. It is up-regulated in neuronal cells of patients suffering from neurodegenerative disorders including Alzheimer's and Parkinson's diseases, where it is found bound to amyloid plaques[7]. An understanding of how this chaperone inhibits protein aggregation has proven elusive. Structural studies are challenged by the fact that αB-crystallin populates a heterogeneous ensemble of inter-converting oligomers at equilibrium, with 95% of the oligomers sized between 20 and 40-mers[8]. Despite this complexity αB-crystallin oligomers possess several remarkably simplifying features. Both solid- and solution-state NMR studies have established that the overall structure adopted by the constituent monomers is essentially independent of oligomer size[9,10]. In addition, we have previously shown that the equilibrium size distribution can be quantitatively explained assuming that both the dimer interface and the interface holding neighboring dimers together are similar in all oligomers[8]. These observations have allowed us to construct structural models of the principally populated oligomers in solution, Fig. 1A[11]. Alternative models of αB-crystallin have also been recently put forward[12,13].

The primary sequence of αB-crystallin and of sHSPs in general can be divided into three parts[14-16], the N- and C-termini and a core domain (Fig. 1A,i). The termini are involved in holding the oligomers together and the motional properties of a highly conserved IxI motif in the C-terminus are thought to play a critical role in regulating the kinetics and thermodynamics of monomer exchange between oligomers[9]. The end of the C-terminus, a region termed the extension (green in Fig. 1A,i), is intrinsically disordered. For example, residues 164-175 were observed in solution ^{1}H NMR spectra using experiments and samples

that were not optimized for large proteins, only possible if this region is highly mobile[17-19]. Of interest, mutations in the C-terminus modulate chaperone activity[20,21] and have been linked to disease[22-24].

When both of the termini are removed the core domain forms β-sheet rich dimers (Fig. 1A,ii) that serve as the 'building blocks' for the oligomeric structures[25,26]. Deletion of the N terminus and the C-terminus past the IxI motif (residues 159-161 in αB-crystallin, Fig. 1A,i) leads to predominantly monomers and dimers in solution, although a significant population of oligomers remains[27]. When crystallized, the IxI residues in this deletion construct form contacts between dimers[27], mimicking an interaction observed in crystal structures of homologous sHSP oligomers[28,29]. Notably, solid-state NMR studies of αB-crystallin comprising full length protein establish that each dimeric unit adopts a similar structure to that in Fig. 1A,ii, with the IxI residues tightly bound to adjacent dimers[10]. In contrast, a different picture has emerged from solution-state NMR where spin relaxation studies of the IxI residues show that they are highly mobile[9]. Indeed, the ^{13}C chemical shifts of the Ile $\delta 1$ carbons in the IxI motif, 12.5 and 12.3 ppm, are consistent with the values observed for a random coil[30]. Although it is clear that in solution the IxI motif is disordered and unbound, paramagnetic relaxation enhancement NMR measurements establish that these residues, nevertheless, are localized to a region proximal to a binding pocket[9] that has been elucidated by solid state NMR and X-ray diffraction studies[10,27]

In order to resolve this apparent discrepancy and to further characterize the dynamics of the IxI residues we have employed a combination of both solution- and solid-state NMR using U-[^{2}H], Ile-[^{13}CH$_3$ $\delta 1$], Leu,Val-[^{13}CH$_3$,^{12}CD$_3$] samples of αB-crystallin. The solution NMR experiments exploit a methyl-TROSY effect that is critical in studies of very high molecular weight proteins (average molecular mass of 580 kDa)[31,32]. Following the elegant work of Reif, Oshkinat and coworkers we have used MAS NMR of samples sedimented by ultracentrifugation and prepared according to the FROSTY protocol[33,34] (referred to as FROSTY-MAS below) to examine both the 'liquid'-and 'solid'-like properties

of the IxI motif of αB-crystallin. By using the same sample labeling for both sets of experiments the solution and solid-state NMR results can be compared directly. Moreover, the extensive protein deuteration that benefits the solution NMR studies is also advantageous in removing unwanted dipolar interactions in the solid-state based experiments. We show here, through a combination of both solution and solid-state NMR techniques, that at temperatures below 0°C the IxI moiety exists in at least two states, corresponding to bound and highly mobile conformations, while above 0°C only the mobile state is observed in NMR spectra. Solution NMR relaxation dispersion studies establish further that the mobile IxI conformation interchanges with a sparsely populated state that, remarkably, has structural features that are similar to those of the bound state that has been characterized previously both by solid-state NMR[10] and X-ray diffraction[27].

Materials and Methods

Protein production and purification

αB-crystallin was prepared by overnight expression in *E.coli* BL21(DE3) cells, 37°C. Cells were harvested and lysed in 20 mM Tris pH 8 buffer in the presence of a protease inhibitor cocktail (Roche). After purification on a Q-column, with protein eluting at 100 mM NaCl[35], the fractions containing αB-crystallin were pooled, concentrated and further purified using an S200 gel filtration column in 150 mM NaCl, 50 mM Tris, pH 8.0. U-^{2}H,Ile-[^{13}CH$_3$-δ1] protein was prepared by growing in D$_2$O and M9 media with [^{12}C,^{2}H] glucose as the sole carbon source and the precursor sodium α-ketobutyrate [^{13}CH$_3$CD$_2$COCO$_2$Na] (60 mg/L) added 1 hour prior to induction[36]. U-^{2}H,Ile-[^{13}CH$_3$-δ1], Leu,Val-[^{13}CH$_3$,^{12}CD$_3$] αB-crystallin was generated as for Ile-labelled protein, with the addition of α-ketoisovalerate [^{13}CH$_3$CD$_3$CDCOCO$_2$Na] (80 mg/L) as described previously[36]. NMR samples in the concentration range 200 μM to 1.5 mM were transferred into a buffer containing 2 mM EDTA, 2 mM NaN$_3$ and 30 mM sodium phosphate in 100% D$_2$O, adjusted to the desired pH

with DCl and NaOD. Samples for solid-state NMR were then mixed with glycerol and further concentrated, as described below.

In order to obtain the assignments of I159δ1, I161δ1, and V169γ1,γ2 methyl groups, as described previously[9], we have used a mutagenesis approach involving the production of I159V/I161V U-^{2}H,Ile-[^{13}CH$_3$-δ1]-αB and I161A/V169S U-^{2}H,Ile-[^{13}CH$_3$-δ1], Leu,Val-[^{13}CH$_3$,^{12}CD$_3$]-αB crystallin samples [9]. Notably, both samples expressed at levels that were comparable to that of the wild type and eluted at the same volume as wild type when purified by size exclusion chromatography. The details of the assignment are provided in Fig. S1.

Solution-state NMR measurements

^{13}C-^{1}H correlation spectra were acquired using Varian NMR spectrometers operating at field strengths of 11.7T (room temperature probe), 14.0T (cryogenically cooled probe) and 18.8T (room temperature probe) over a range of pHs (5-9) and temperatures (5-50°C) using experiments that exploit a methyl-TROSY effect, described in detail previously[31,32,37-39]. Relaxation data were recorded on samples at pH 5 where the effects of chemical exchange are maximal. Data showing the same exchange process were obtained at pH 7, though the effects were significantly more challenging to quantify because the population of the excited state is considerably lower. All data were processed using the NMRPipe program[40].

^{1}H transverse relaxation rates, with selection for the slowly relaxing methyl proton component, were measured as described previously[41] over a range of temperatures extending from 5-50°C, pH 5, 14.0T. Similarly, ^{1}H and ^{13}C single quantum relaxation dispersion experiments[42] were performed over the same temperature range, pH 5, 14.0T and 18.8T. A constant time CPMG relaxation delay of 40 ms was employed with 17 CPMG frequencies in the range 50-2000 Hz, including several repeat values for error analysis[43]. $R_{2,eff}(\nu_{CPMG})$ values were obtained via the relation $R_{2,eff}(\nu_{CPMG}) = -\dfrac{1}{T_{relax}} \ln \dfrac{I(\nu_{CPMG})}{I_0}$, where $I(\nu_{CPMG})$ and I_0 are peak intensities with and without the 40 ms constant-time CPMG delay, respectively, and

ν_{CPMG} is the inverse of twice the delay between successive 180° pulses. Values of exchange

parameters were extracted from fits of $R_{2,eff}(\nu_{CPMG})$ profiles to a two-site exchange model, as

described previously[44] using the in-house written program CATIA

(http://abragam.med.utoronto.ca/software.html)[44,45].

Spin-state selective methyl ^{13}C relaxation dispersion experiments were performed at

50°C, pH 5 following an approach described in detail previously[45]. A constant time CPMG

element of 40 ms was used, along with 21 CPMG frequencies in the range 50 to 2000 Hz.

Errors in $R_{2,eff}$ were estimated on the basis of repeat ν_{CPMG} values[43]. Dispersion data were

fitted to a two-site exchange process using a relaxation model that has been described[9,45].

Central to the work here is that residue specific values for $S^2 \tau_c$ are obtained, where S^2 is the

square of an order parameter quantifying the amplitude of motion of the methyl rotation axis

and τ_c is the correlation time for the assumed isotropic molecular tumbling. Thus, it is

possible to establish the relative mobilities of corresponding methyl groups in the ground

and excited states, as discussed below.

Solid-state NMR measurements

αB-crystallin protein samples were prepared for solid-state NMR analyses according

to the 'FROSTY' procedure of Mainz et al[33]. In brief, labelled αB-crystallin was concentrated

in a 100 kDa ultrafiltration membrane to a volume of 36 μl. An equal volume of 40% glycerol

was added once a concentration of approximately 50 mg/ml was obtained. The sample

volume was then reduced by half, yielding a solution of 50 mg/ml protein in 20% v/v

glycerol, in the NMR buffer described above. The sample (final volume 36 μl) was

subsequently packed into a 3.2 mm thin walled MAS rotor using centrifugation.

Solid-state NMR spectra were acquired on a narrow-bore Varian VNMRS

spectrometer operating at a field strength of 11.7T. All experiments were performed using a

triple resonance T3 MAS probe operating in 2-channel mode. In all cases the MAS frequency

was 12 kHz, and ^{1}H decoupling during ^{13}C evolution, detection and mixing periods was

achieved with a 120 kHz ^{1}H two-pulse phase modulated (TPPM) scheme[46]. The sample temperature under MAS conditions was calibrated using the ^{207}Pb chemical shift of solid PbNO$_3$[47]. At -20 and +20°C respectively, 1 and 3°C of sample heating was observed.

1D ^{13}C spectra were obtained under MAS using either INEPT or CP transfer from ^{1}H, with each spectrum taking approximately 2 hours to acquire. For CP experiments ^{13}C and ^{1}H field strengths of approximately 50 kHz and 62 kHz respectively were used, with contact times of 1.2-1.4 ms and a small linear ramp on the ^{13}C channel[48]. 2D ^{13}C-^{13}C correlation spectra were recorded using a finite-pulse radio-frequency driven recoupling (RFDR)[49] sequence for ^{13}C recoupling, with a mixing period of 8 ms and 25 kHz ^{13}C fields during RFDR. The transmitter was centred within the aliphatic region for RFDR experiments, and 40 t_1 points (sweep width of 3770 Hz) were acquired in the indirect dimension, with a total experiment time of 25 hours. 2D ^{1}H-^{13}C HETCOR spectra were obtained using either CP or INEPT transfer following the t_1 (^{1}H evolution) period. ^{1}H homonuclear decoupling was employed during the t_1 period of the CP-based experiment using a frequency-switched Lee-Goldberg sequence[50] at a field strength of 80kHz. 64 t_1 points were acquired, with a sweep width of 9600 Hz in the indirect dimension and a total experiment time of 18 hours. A scaling factor of $1/\sqrt{3}$ was applied to the ^{1}H chemical shift dimension of the FSLG-CP HETCOR, as previously described[51].

Results and Discussion

As described in the Introduction, the IxI motif in the C-terminal region of αB-crystallin, Fig. 1A, plays a critical role in controlling the kinetics and thermodynamics of subunit interchange between the ensemble of oligomeric structures that this protein populates in solution[9] (see below). It is important, therefore, to reconcile the differences between solution-state NMR results establishing that the Ile residues are highly mobile and

solid-state NMR data showing that the IxI motif is in a bound conformation, and hence (relatively) rigid. To this end we have recorded both solution- and solid-state NMR spectra, Fig. 1B, using samples prepared with identical labeling to serve as a starting point for further analysis of the dynamics of this important region[19-24] (see below). FROSTY-MAS HETCOR experiments using cross-polarization (CP) for magnetization transfer have been recorded previously on samples of αB-crystallin at low temperatures[10,33]. We show here that a multiple temperature analysis of such HETCOR spectra, measured with CP and INEPT magnetization transfers, and solution HMQC data sets allows insight into how the structures observed by solid-state NMR relate to those populated in solution, which are the more physiologically relevant.

In a previous publication we noted that there are four very intense correlations in the Ile, Leu, Val ^{13}C,^{1}H solution HMQC spectrum of αB-crystallin[9], derived from I159δ1, I161δ1, and V169γ1,γ2 methyl groups localized to the C-terminus of the protein, Fig. 1B,I (see Fig. S1). Interestingly, none of the N-terminal I residues (I3δ1, I5δ1, I10δ1) give rise to cross peaks of comparable intensities, suggesting that they are much less dynamic. The proton and carbon spins from each of I159δ1, I161δ1, and V169γ1,γ2 methyl groups have relaxation rates and chemical shifts that are consistent with a disordered region[9]. The intensities of the V169γ resonances increase with temperature in a manner consistent with increased tumbling rates. In contrast, I159δ1,I161δ1 peak intensities increase much less significantly and in fact decrease at higher temperatures, consistent with a conformational exchange process that becomes more significant with increasing temperature[9]. The observed intensity *vs* temperature profile for these Ile and Val residues does not reflect different temperature dependencies for ^{1}H T_1 values as measurements establish essentially identical relative values at 25 and 45°C, $R_2^{Val} / R_2^{Ile} = 2.0 \pm 0.1$. In fact, as we show below, both the ^{1}H and ^{13}C linewidths for I159δ1,I161δ1 are significantly larger than for V169γ at 50°C, with the differences becoming pronounced already at 30°C.

By means of comparison we have also recorded ^{13}C detected FROSTY-MAS[33] based HETCOR spectra where the ^{1}H to ^{13}C polarization transfer step is carried out using an INEPT scheme[52] ('MAS INEPT HETCOR', Figure 1B,ii). The INEPT transfer will preferentially 'select' flexible regions so that the solid-state data set recorded in this manner is very similar to the solution spectrum, with intense correlations observed for I159δ1, I161δ1 and Val169γ methyl groups. All correlations increase significantly with temperature from -22°C to 0°C. Interestingly, both Ile peaks decrease in intensity from 0°C to 30°C, consistent with an exchange process, as observed in the solution state, although in solution the increased line broadening from exchange is compensated to some extent by more rapid overall tumbling as the temperature increases. FROSTY-MAS HETCOR spectra have also been obtained with ^{1}H to ^{13}C cross-polarization[48,51] ('MAS FSLG-CP HETCOR', Figure 1B,iii) that are very similar to those previously recorded by Reif and coworkers[33]. Notably, at -22°C a resonance from I159δ1 is observed at 9.5 ppm, in contrast to 12.3 ppm for the corresponding peak in the solution state or in FROSTY spectra recorded with INEPT magnetization transfer. Cross peaks are observed between I159δ1 and I133δ1,V93γ methyl groups in 2D [13]C-^{13}C RFDR spectra[49] (Fig. S2), consistent with X-ray structures of a number of sHSPs[27-29] and with a recent solid-state NMR derived model of the αB-crystallin core dimer[10] where the IxI motif is rigidly attached to an adjacent dimer in the structure. The FROSTY-MAS spectra presented here thus provide strong evidence for the IxI moiety populating two conformations at low temperature (-22°C), one that is tightly bound and a second state that is disordered and very similar to the major conformation in solution, that is the dominant form at higher temperatures.
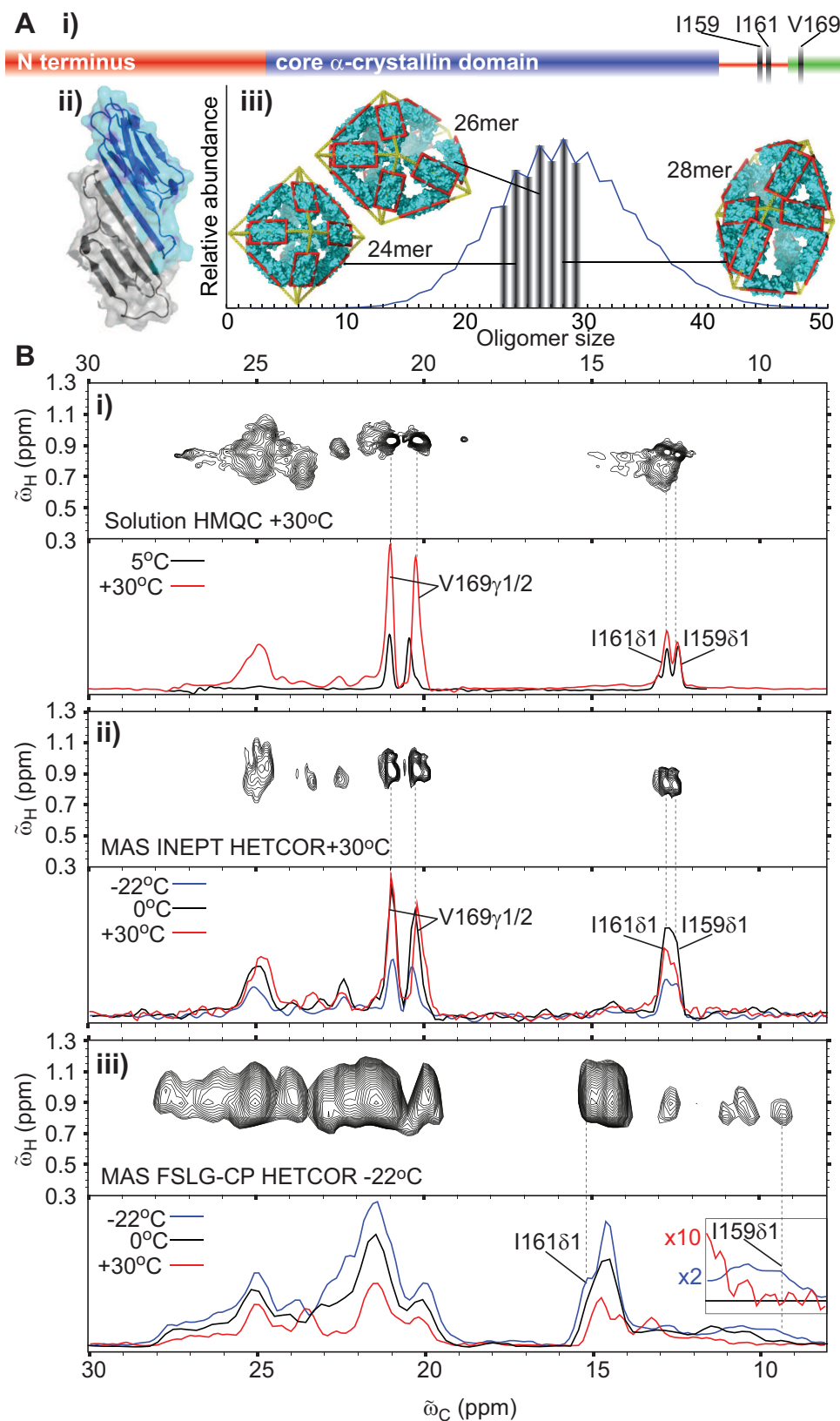
Figure 1: A) i) The sequence of αB-crystallin can be separated into three regions, an N-terminus (1-57), the core α-crystallin (aC) domain and the C-terminus (149-175). ii) The core domain adopts a β-

sheet rich fold which dimerizes. The basic building block dimeric structure of αB-crystallin, lacking the N and C termini, is illustrated (PDB accession code 2wj7[25]). iii) The core dimer structure assembles into a wide range of inter-converting oligomers in solution[8]. Structural models of the 23mer-29mer (bars) have recently been determined[11]. B) i) The solution NMR spectrum of U-[^{2}H], Ile-[$^{13}CH_3$ δ1], Leu,Val-[$^{13}CH_3,^{12}CD_3$] αB-crystallin, 30°C, 14.0T, pH 7 with prominent resonances from the C-terminal methyl groups of I159δ1, 161δ1 and V169γ1/γ2. Correlations for all 9 isoleucine residues in αB-crystallin are observed in spectra recorded on samples with only Ile labeling[9] with only a single resonance obtained for each Iδ1. The upfield correlation observed for I159δ1 in the CP-MAS spectrum, -22°C, at 9.5 ppm (see iii) is shifted to 12.3 ppm in solution; a peak is not observed at 9.5 ppm. ii) The FROSTY-MAS[33] spectrum of U-[^{2}H], Ile-[$^{13}CH_3$ δ1], Leu,Val-[$^{13}CH_3,^{12}CD_3$] αB-crystallin, 30°C pH 7, 11.7T, with ^{1}H to ^{13}C polarization transfer achieved via INEPT [52] is very similar to the solution data set. iii) As in (ii) but with polarization transfer via CP[51], -22°C, 11.7T. Notably, resonances from I159δ1 and I161δ1 at ϖ_C values of 9.5 and 15 ppm, respectively, can be clearly discerned. At temperatures of 0°C and higher this resonance for I159δ1 is no longer observed. While the intensity of the peak derived from I161δ1 appears to decrease with temperature as well this is difficult to conclude with certainty because of the appreciable overlap in this region.

In order to probe the conformational exchange process involving the Ile residues (see above) in more detail and to understand how the inter-converting states may be related structurally we have carried out solution state Carr-Purcell-Meiboom-Gill (CPMG)[53,54] relaxation dispersion (RD) experiments, Fig. 2. The single-quantum ^{13}C RD profiles[42] obtained for both I159δ1 and I161δ1 show the characteristic signature of exchange with effective transverse relaxation rates, $R_{2,eff}$, decreasing as a function of increasing pulse rate (ν_{CPMG}). In contrast, the RD curves for the two methyl resonances from V169 are independent of ν_{CPMG}, consistent with the absence of chemical exchange or with a scenario where there is little chemical shift difference between exchanging states. A detailed analysis of the RD data presented previously[9] indicates that the major conformation, corresponding to the dynamic unbound IxI state, exchanges with a second conformer which has a maximum fractional population of 2% at 50°C, pH 7, increasing with decreasing pH [9]. The effects of exchange as a function of both pH and temperature and quantified by both NMR and mass spectrometry have been described previously[8,9], establishing that the same exchange process manifests over the complete pH and temperature range examined. For completeness here, Fig. S3

shows ^{1}H 1D, ^{13}C-edited NMR spectra recorded at a number of temperatures and pHs, with exchange contributions increasing at the lower pH values and at higher temperatures. As described in Materials and Methods and below we have carried out further detailed relaxation dispersion experiments at pH 5 to maximize the observed exchange effects.

At the time of our initial relaxation experiments[9] we were not able to determine the Ile ^{13}Cδ1 chemical shifts in the sparsely populated state since only the absolute values of the differences in shifts between exchanging conformers are available from relaxation dispersion data sets. The structural features of the IxI motif in the bound conformation were thus not established. Additionally, no information was available concerning the motional properties of IxI in the excited state. This information is critical to our model of subunit exchange that is described below.

With the recent development of $R_{1\rho}$ experiments that provide signs of chemical shift differences between exchanging states even in cases where large differences in intrinsic relaxation rates are present[55] (see below) we can now establish that the ^{13}C chemical shifts of I159δ1 and I161δ1 in the 'excited' state are 10.5 and 14.1 ppm, respectively. These shifts are similar to those for the bound state from solid-state NMR at -22°C (9.5 and 15 ppm respectively, Fig. 1B,iii), indicating that the sparsely populated state may resemble the bound conformer observed by solid-state NMR[10].
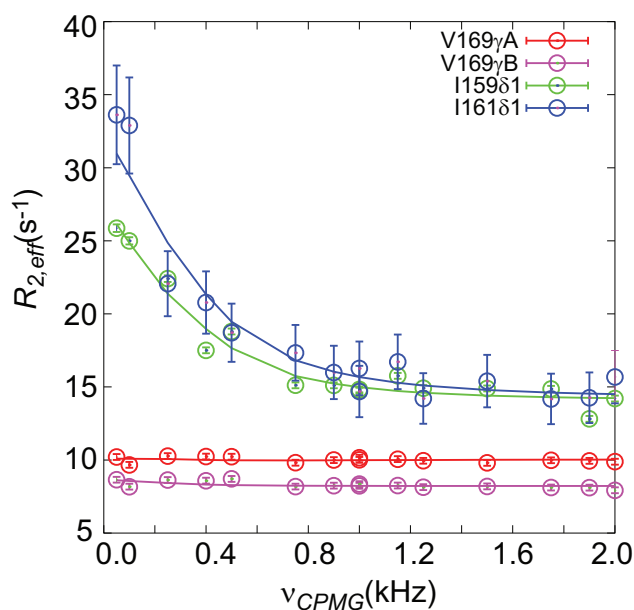
Figure 2: Relaxation dispersion NMR spectroscopy reveals millisecond timescale dynamics in the C-terminus of αB-crystallin. **A)** Single quantum ^{13}C relaxation dispersion curves of the four C-terminal methyl resonances[42], I159δ1, I161δ1, V169γ1/γ2, pH 4.7, 50°C, 18.8T. Relaxation dispersion curves of V169γ1/γ2 do not show evidence of exchange on the ms time-scale. In contrast, the corresponding curves for I159δ1 and I161δ1 reveal a strong contribution from the effects of millisecond dynamics. Analysis of the data using a two-state exchange model, as described previously[9], reveals an additional sparsely populated conformational state with a fractional population of 3% and lifetimes for the ground and excited states of 38 and 1 ms, respectively[9]. The sparsely populated state has been shown to regulate the subunit exchange process[9]. Methyl groups for V169 have not been stereospecifically assigned and hence are denoted 'A', 'B'.

As described above, previous solution NMR studies have established that the IxI ground state is highly dynamic[9]. Further evidence is derived from the relative intensities of the ^{13}C methyl multiplet components recorded in an F_1-coupled HSQC data set. In such a spectrum four individual components of the $^{13}CH_3$ group are observed corresponding to the ^{13}C spin coupled to protons either all 'up' (ααα) or 'down' (βββ), outer multiplet components, or to protons in the '2 up/1 down' (ααβ) or 2 'down/1 up' (ββα) states, inner components. For a highly dynamic methyl group there is little difference in transverse relaxation rates of each of the carbon lines so that a 3:1:1:3 multiplet structure is predicted[32]. In contrast, in the slow tumbling limit the net ^{13}C-^1H dipolar interaction is 3 fold larger for the outer lines,

leading to a decay rate that is approximately 9 times more rapid than for the inner components[56]. Similar ratios of outer to inner components, 3.1/1 - 2.9/1, are found for both I159δ1 and I161δ1, confirming the highly dynamic nature of these residues in the ground state, Fig. 3A. To obtain insight into the motional properties of these isoleucines in the excited state we have recorded the decay of methyl ^{1}H transverse magnetization[41], $R_{2,1H}$, as a function of temperature, Fig. 3B. As a control we have also measured $R_{2,1H}$ values for the methyl protons of V169. These were found to decrease with temperature, as expected based on decreasing solution viscosity and enhanced molecular tumbling. Between 0 and 20°C, proton relaxation rates for I159δ1 and I161δ1 methyl groups also followed this trend. Above 20°C, however, $R_{2,1H}$ values were found to increase significantly and at 50°C ^{1}H transverse relaxation rates for the δ methyls of I159/I161 were approximately 3 fold larger than for the protons from methyls of V169. The increase in relaxation rates (minimum in R_2 *vs* temperature profile, Fig. 3B) coincides precisely where the effects of chemical exchange become observable via ^{13}C CPMG RD. Moreover, ^{1}H CPMG RD profiles showed essentially no dependence on ν_{CPMG} over the complete temperature range, Fig. S4. The simplest interpretation of the Ile relaxation data is, therefore, that the ^{1}H R_2 rate can be described in terms of a population weighted average of ground and excited state relaxation rates, with the population of the excited state increasing with temperature and with R_2 values in the excited conformer greatly exceeding those in the ground state.
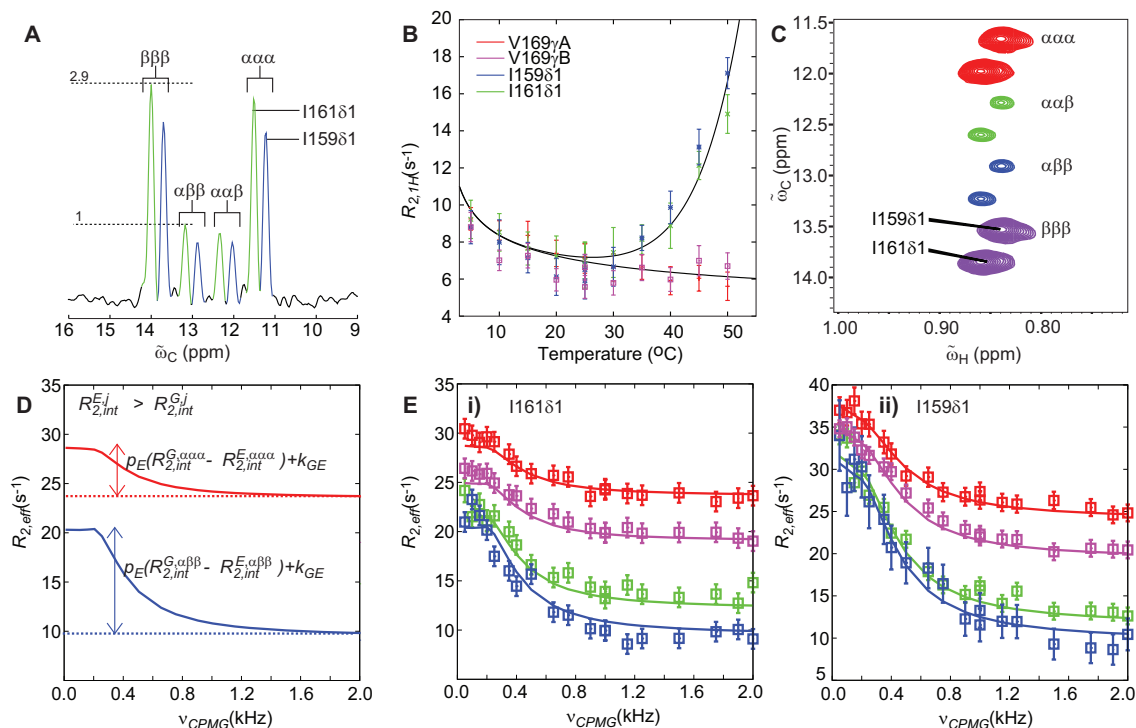
Figure 3: A) Trace through a ^{1}H-^{13}C HSQC spectrum of U-[^{2}H], Ile-[^{13}CH$_3$ δ1], Leu,Val-[^{13}CH$_3$,^{12}CD$_3$] αB-crystallin, 45°C, 14.0T, pH 5, recorded without proton decoupling during acquisition of carbon chemical shift. The resonances from I159δ1 and I161δ1 are approximately in the ratio 3:1:1:3. **B)** ^{1}H R_2 rates as a function of temperature for I159δ1, I161δ1 and V169γ1/γ2 (stereospecific assignments of V169 methyl groups are not available and hence V169 methyls are denoted 'A', 'B'). Rates are measured as described previously[9]. $R_{2,1H}$ values for V169 decrease in a manner consistent with decreasing solution viscosity. Similarly, $R_{2,1H}$ rates for I159δ1 and I161δ1 decrease with increasing temperature in the temperature range 0°C-20°C, while at higher temperatures the rates increase rapidly. Solid lines in the figure are meant to guide the eye. **C)** 2D ^{13}C-^{1}H correlation map, corresponding to the first plane of a spin-state selective CPMG RD experiment[45,57], with the four spin-state selective multiplet components observed. The ^{1}H spin-states associated with each multiplet line are as indicated with α and β corresponding to ^{1}H spin up and down. **D)** Fits of relaxation dispersion curves of the four separated ^{13}C methyl multiplet components can establish the dynamic properties of the sparsely populated ('invisible') state, as described in detail previously[45] and summarized in the text. A schematic illustrating that the sizes of the dispersion profiles (arrows) for the outer lines (only the most upfield line is shown) are smaller than for the inner lines (only one of the two is indicated) in the case where the methyl probe in the excited state is less dynamic than in the ground conformation. **E)** Relaxation dispersion curves of the four separated components for Ile 159δ1 (i) and I161δ1 (ii) pH 5, 40°C, 18.8T, analyzed and fit (solid lines) as described previously[45]. The sizes of dispersion profiles derived from the inner lines are larger than from the outer lines for both residues, corresponding to $R_{2,int}^{E,j} > R_{2,int}^{G,j}$. Data were recorded at pH 5 where the population of the excited state, and so the magnitude of the difference in relaxation between the outer and inner lines, is maximal.

More quantitative information can be obtained by recording spin-state selective ^{13}C methyl RD profiles where each of the four lines of the multiplet component, Fig. 3C, gives rise to a separate dispersion profile[45]. In the absence of relaxation differences between ground and excited states the dispersion profiles for each of the four lines differ only by a vertical displacement. In contrast, when the relaxation rates for the ^{13}C methyl spin in question are different in each of the inter-converting states, distinct profiles are observed that cannot be superimposed, as illustrated schematically in Fig. 3D[45]. The main features in this figure can be understood most simply by considering a two-state exchanging spin system in moderately slow exchange. In the limit that the CPMG pulsing rate is very slow, $\nu_{CPMG} \to 0$, $R_{2,eff}$ rates for each of the four lines are given by $R_{2,eff}^{G,j}(0) = k_{GE} + R_{2,int}^{G,j}$, $j \in \{\alpha\alpha\alpha, \alpha\alpha\beta, \alpha\beta\beta, \beta\beta\beta\}$, where $R_{2,int}^{G,j}$ is the intrinsic ^{13}C methyl j spin-state transverse relaxation rate for the ground state conformer and k_{mn} is the rate of exchange from state m to n. In the case where pulsing is rapid $\nu_{CPMG} \to \infty$ the value of $R_{2,eff}$ becomes the population weighted average of relaxation rates in each of the inter-converting states (assuming that exchange is faster than $|R_{2,int}^{G} - R_{2,int}^{E}|$), $R_{2,eff}^{G,j}(\infty) = p_G R_{2,int}^{G,j} + p_E R_{2,int}^{E,j}$, where p_G and $p_E = 1-p_G$ are the fractional populations of the ground and excited states, respectively. The 'size' of the dispersion profile (arrow in Fig. 3D) is thus given by $R_{2,eff}^{G,j}(0) - R_{2,eff}^{G,j}(\infty) = k_{GE} + p_E(R_{2,int}^{G,j} - R_{2,int}^{E,j})$. Noting that in the macromolecule limit (such as for proteins) the outer multiplet components relax more rapidly than the inner lines, $R_{2,int}^{\alpha\alpha\alpha}, R_{2,int}^{\beta\beta\beta} > R_{2,int}^{\alpha\alpha\beta}, R_{2,int}^{\alpha\beta\beta}$ [45,56] (see above) and assuming that $R_{2,int}^{E,j} > R_{2,int}^{G,j}$ the schematic shown in Fig. 3D is obtained where dispersion profiles from the inner lines are larger than those from the outer components. In contrast, when $R_{2,int}^{E,j} < R_{2,int}^{G,j}$ the situation is reversed. Figs. 3Ei,ii show RD profiles for each of the four lines for I159δ1 (i) and I161δ1 (ii) (18.8T, 50°C) and it is clear that substantial differences in the curves are obtained, exactly as predicted in Fig. 3D. Even without a detailed analysis of the data it follows simply by inspection that the excited state conformation is one in which the Ile residues are very much less mobile than in

the populated ground state. Fits (solid lines) to the experimental data (squares), measured at fields of 11.7, 14.0 and 18.8T, using a two-site model of exchange were performed as described in detail previously[45], assuming that both Ile residues report on the same exchange process (same populations and rates). An important parameter obtained from the fit is $\Delta(S^2\tau_c) = (S^2\tau_c)_E - (S^2\tau_c)_G$ where S^2 is a methyl axis order parameter and τ_c is the (assumed isotropic) correlation time in either the excited (E) or the ground (G) state. Values of $\Delta(S^2\tau_c)$ of +180 and +100 ns were obtained for I159δ1 and I161δ1 respectively, confirming that the excited state is indeed bound.
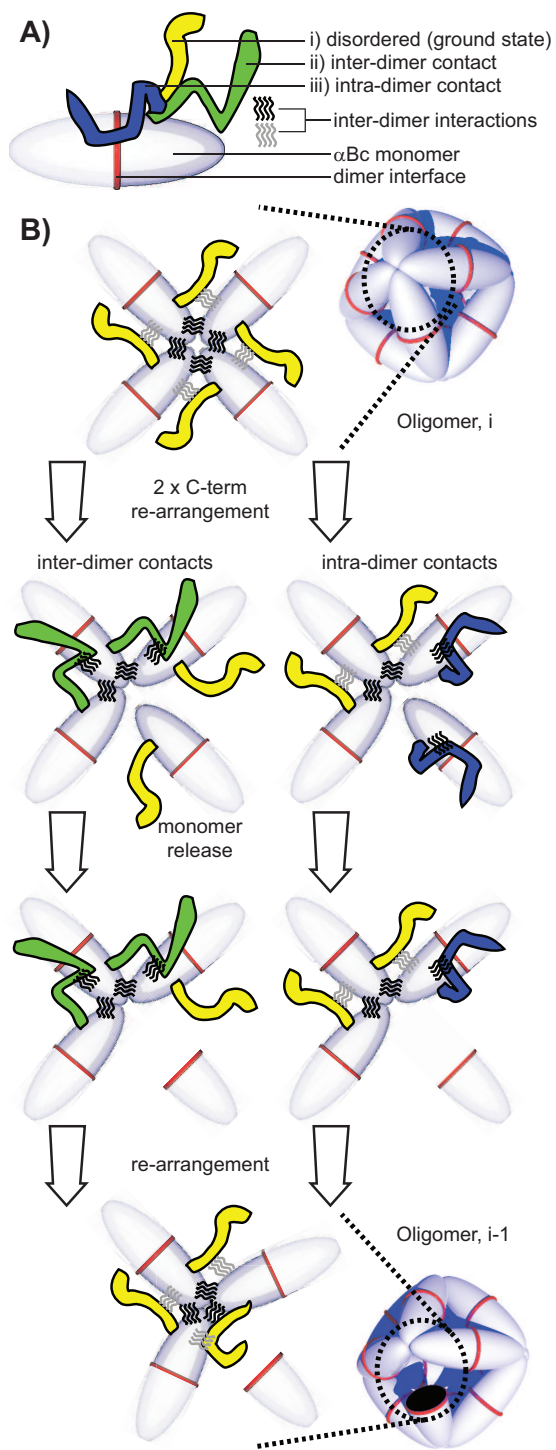
Figure 4: A microscopic mechanism for monomer dissociation and subunit exchange of αB-crystallin oligomers. Although the model is illustrated for an octahedral 24mer (Oligomer, i) it applies equally to any polyhedral structure where an integer number of monomers come together about a vertex. Details are given in the text.

The formation of the excited state has previously been linked with the process of subunit exchange in αB-crystallin[9]. The finding that it is bound leads to a straightforward model that can explain how subunit exchange occurs in terms of the formation and breaking of specific interactions within oligomers. Our previous studies have established that monomers of αB-crystallin (half ellipses in Figure 4) are held in place within a given oligomer by two types of interactions[8]. The first is intra-dimer, depicted in our model in Figure 4 by a red ring, while the second class is inter-dimer, denoted by wavy lines (black or grey). A model that assumes only these two classes of interactions, that are essentially independent of oligomer size, quantitatively accounts for the oligomeric distributions observed over a wide range of solution conditions, as measured by mass spectrometry[8]. While the structural basis of the intra-dimer interactions is well understood[10,25-27], the atomic contacts that constitute the inter-dimer interface are presently less well known. Previous work using NMR paramagnetic relaxation enhancement measurements has shown that the intrinsically disordered 'ground state' of the C-terminus (yellow) makes transient contacts with a specific hydrophobic groove on adjacent monomers[9], contributing to the stabilization of the inter-dimer interface (denoted by grey wavy lines in Figure 4). Other interactions both between monomers or involving the N-terminus have also been identified as contributing towards the stability of this interface[27] and are denoted by black wavy lines.

Using results from a combination of mass spectrometry[8], X-ray diffraction[25] and NMR[9] analyses we concluded previously[11] that 1) all monomers must be in equivalent environments, 2) oligomers are comprised of dimeric building blocks, 3) each monomer is connected to an oligomer via a pair of C-terminal 'cross-linking' interactions that must be broken prior to monomer release and 4) models of oligomers could be constructed based on polyhedral scaffolds. Taken together, in concert with experimental data from ion-mobility mass spectrometry and electron microscopy[11], the structure of a 24mer can be described by an octahedron, shown schematically in Figure 4B ("Oligomer i"). Focusing on a single polyhedral vertex (they are all the same) it is clear that four dimers come together with each

specific monomer interacting with its two immediate neighbors (black and grey wavy lines). In order for a monomer to dissociate from the oligomer, therefore, both of the 'immediate neighbor' stabilizing interactions must be broken. Supporting this notion, NMR relaxation dispersion and mass spectrometry kinetic data[9], can be reconciled assuming that the dissociation process involves the simultaneous rearrangement of a pair of C-termini (including IxI motifs) as depicted in the model described by Figure 4. Here, disordered C-termini, corresponding to ground states (yellow), simultaneously form ordered low populated conformers, denoted here as either inter-dimer (green, left side) or intra-dimer (blue, right side), leading to the release of the C-terminal interactions. In this model formation of either two inter- or two intra- C-terminal interactions, or a mixture of both, corresponding to an ordering of the IxI region, results in a distortion of the oligomer, leading to the breaking of interactions holding a specific monomer in place and thereby facilitating its departure. Subsequently the structure rearranges so that all monomers occupy an identical environment. The model thus provides a link between the macroscopic process of subunit exchange and microscopic fluctuations of the C-terminal IxI.

Concluding Remarks

The present study establishes that at least two distinct structural environments are adopted by the C-terminal IxI residues of αB-crystallin, one free and one bound, with relative populations varying substantially with temperature. While both disordered and bound states are seen at low temperatures, above $0°C$ only the highly mobile conformation is appreciably populated. Interestingly, this 'ground' state conformer exchanges with a second sparsely populated state where the IxI moiety is much more rigid ('bound') and where the [13]C Ile $\delta 1$ methyl chemical shifts are similar to those reported from a solid state NMR study of αB-crystallin at low temperature[10]. The excited state has been shown previously to play an important role in controlling the kinetics and thermodynamics of subunit interchange between different oligomers and the resulting particle size distribution[8,9]. Intriguingly, the

present study has established that the excited state conformation of the IxI motif shares several important features with the 'bound' state structure reported from both solid-state NMR and X-ray methods[10,27], leading to a proposed mechanism for the subunit exchange process. The complementary of the information derived here from both solid- and solution-state NMR experiments is important for elucidating the detailed mechanism by which dynamics are able to regulate the function of this important molecule.

Supporting Information

Figures showing (i) assignment of I159/161 $\delta 1$ methyl groups, (ii) solid state NMR spectra, (iii) effects of pH and temperature on I159/161 and V169 ^{1}H NMR spectra and (iv) ^{1}H/^{13}C CPMG relaxation dispersion profiles of αB-crystallin. This material is available free of charge via the Internet at http://pubs.acs.org.

Author Information Notes

Corresponding author emails: kay@pound.med.utoronto.ca; ajb204@gmail.com

Acknowledgments

Abbreviations

NMR, nuclear magnetic resonance; CPMG, Carr-Purcell-Meiboom-Gill; MAS, magic angle spinning; FROSTY, Freezing Rotational diffusion of Protein Solutions at low Temperature and high viscositY; CP, cross polarization; INEPT, Insensitive Nuclei Enhanced by Polarization Transfer; FSLG, frequency switched Lee-Goldberg; HMQC, Heteronuclear multiple quantum coherence; HETCOR, heteronuclear correlation.

References

(1)   Baldwin, A. J.; Knowles, T. P.; Tartaglia, G. G.; Fitzpatrick, A. W.; Devlin, G. L.; Shammas, S. L.; Waudby, C. A.; Mossuto, M. F.; Meehan, S.; Gras, S. L.; Christodoulou, J.; Anthony-Cahill, S. J.; Barker, P. D.; Vendruscolo, M.; Dobson, C. M. *J Am Chem Soc* **2011**, *133*, 14160-3.

(2)   Hartl, F. U.; Bracher, A.; Hayer-Hartl, M. *Nature* **2011**, *475*, 324-32.

(3)   Haslbeck, M.; Franzmann, T.; Weinfurtner, D.; Buchner, J. *Nat Struct Mol Biol* **2005**, *12*, 842-6.

(4)   Balch, W. E.; Morimoto, R. I.; Dillin, A.; Kelly, J. W. *Science (New York, N.Y* **2008**, *319*, 916-9.

(5)   Richter, K.; Haslbeck, M.; Buchner, J. *Mol Cell* **2010**, *40*, 253-66.

(6)   Ecroyd, H.; Carver, J. A. *Cell Mol Life Sci* **2009**, *66*, 62-81.

(7)   Shinohara, H.; Inaguma, Y.; Goto, S.; Inagaki, T.; Kato, K. *J Neurol Sci* **1993**, *119*, 203-8.

(8)   Baldwin, A. J.; Lioe, H.; Robinson, C. V.; Kay, L. E.; Benesch, J. L. *J Mol Biol* **2011**, *413*, 297-309.

(9)   Baldwin, A. J.; Hilton, G. R.; Lioe, H.; Bagneris, C.; Benesch, J. L.; Kay, L. E. *J Mol Biol* **2011**, *413*, 310-20.

(10)   Jehle, S.; Rajagopal, P.; Bardiaux, B.; Markovic, S.; Kuhne, R.; Stout, J. R.; Higman, V. A.; Klevit, R. E.; van Rossum, B. J.; Oschkinat, H. *Nat Struct Mol Biol* **2010**, *17*, 1037-42.

(11)   Baldwin, A. J.; Lioe, H.; Hilton, G. R.; Baker, L. A.; Rubinstein, J. L.; Kay, L. E.; Benesch, J. L. *Structure* **2011**, *19*, 1855-63.

(12)   Braun, N.; Zacharias, M.; Peschek, J.; Kastenmuller, A.; Zou, J.; Hanzlik, M.; Haslbeck, M.; Rappsilber, J.; Buchner, J.; Weinkauf, S. *Proc Natl Acad Sci U S A* **2011**, *108*, 20491-6.

(13)   Jehle, S.; Vollmar, B. S.; Bardiaux, B.; Dove, K. K.; Rajagopal, P.; Gonen, T.; Oschkinat, H.; Klevit, R. E. *Proc Natl Acad Sci U S A* **2011**, *108*, 6409-14.

(14)   Basha, E.; O'Neill, H.; Vierling, E. *Trends Biochem Sci* **2011**, *37*, 106-17.

(15)   Clark, A. R.; Lubsen, N. H.; Slingsby, C. *Int J Biochem Cell Biol* **2012**, *44*, 1687–1697.

(16)   Hilton, G. R.; Lioe, H.; Stengel, F.; Baldwin, A. J.; Benesch, J. L. *Topics in Current Chemistry: Molecular Chaperones* **2012**, *doi: 10.1007/128_2012_324*.

(17)   Carver, J. A.; Aquilina, J. A.; Truscott, R. J.; Ralston, G. B. *FEBS Lett* **1992**, *311*, 143-9.

(18)   Ghahghaei, A.; Rekas, A.; Carver, J. A.; Augusteyn, R. C. *Mol Vis* **2009**, *15*, 2411-20.

(19)   Treweek, T. M.; Rekas, A.; Walker, M. J.; Carver, J. A. *Exp Eye Res* **2010**, *91*, 691-9.

(20)   Pasta, S. Y.; Raman, B.; Ramakrishna, T.; Rao Ch, M. *Mol Vis* **2004**, *10*, 655-62.

(21)   Hayes, V. H.; Devlin, G.; Quinlan, R. A. *J Biol Chem* **2008**, *283*, 10500-12.

(22)   Inagaki, N.; Hayashi, T.; Arimura, T.; Koga, Y.; Takahashi, M.; Shibata, H.; Teraoka, K.; Chikamori, T.; Yamashina, A.; Kimura, A. *Biochem Biophys Res Commun* **2006**, *342*, 379-86.

(23)   Pilotto, A.; Marziliano, N.; Pasotti, M.; Grasso, M.; Costante, A. M.; Arbustini, E. *Biochem Biophys Res Commun* **2006**, *346*, 1115-7.

(24)   Devi, R. R.; Yao, W.; Vijayalakshmi, P.; Sergeev, Y. V.; Sundaresan, P.; Hejtmancik, J. F. *Mol Vis* **2008**, *14*, 1157-70.

(25)   Bagneris, C.; Bateman, O. A.; Naylor, C. E.; Cronin, N.; Boelens, W. C.; Keep, N. H.; Slingsby, C. *J Mol Biol* **2009**, *392*, 1242-52.

(26)   Clark, A. R.; Naylor, C. E.; Bagneris, C.; Keep, N. H.; Slingsby, C. *J Mol Biol* **2011**, *408*, 118-34.

(27)   Laganowsky, A.; Benesch, J. L.; Landau, M.; Ding, L.; Sawaya, M. R.; Cascio, D.; Huang, Q.; Robinson, C. V.; Horwitz, J.; Eisenberg, D. *Protein Sci* **2010**, *19*, 1031-43.

(28)   Kim, K. K.; Kim, R.; Kim, S. H. *Nature* **1998**, *394*, 595-9.

(29)   van Montfort, R. L.; Basha, E.; Friedrich, K. L.; Slingsby, C.; Vierling, E. *Nat Struct Biol* **2001**, *8*, 1025-30.

(30)   Hansen, D. F.; Neudecker, P.; Kay, L. E. *J Am Chem Soc* **2010**, *132*, 7589-91.

(31)   Sprangers, R.; Kay, L. E. *Nature* **2007**, *445*, 618-22.

(32)   Tugarinov, V.; Hwang, P. M.; Ollerenshaw, J. E.; Kay, L. E. *J Am Chem Soc* **2003**, *125*, 10420-8.

(33)   Mainz, A.; Jehle, S.; van Rossum, B. J.; Oschkinat, H.; Reif, B. *J Am Chem Soc* **2009**, *131*, 15968-9.

(34)   Bertini, I.; Luchinat, C.; Parigi, G.; Ravera, E.; Reif, B.; Turano, P. *Proc Natl Acad Sci U S A* **2011**, *108*, 10396-9.

(35)   Meehan, S.; Knowles, T. P.; Baldwin, A. J.; Smith, J. F.; Squires, A. M.; Clements, P.; Treweek, T. M.; Ecroyd, H.; Tartaglia, G. G.; Vendruscolo, M.; Macphee, C. E.; Dobson, C. M.; Carver, J. A. *J Mol Biol* **2007**, *372*, 470-84.

(36)   Ruschak, A. M.; Kay, L. E. *J Biomol NMR* **2010**, *46*, 75-87.

(37)   Sprangers, R.; Velyvis, A.; Kay, L. E. *Nat Methods* **2007**, *4*, 697-703.

(38)   Tugarinov, V.; Sprangers, R.; Kay, L. E. *J Am Chem Soc* **2007**, *129*, 1743-50.

(39)   Ollerenshaw, J. E.; Tugarinov, V.; Kay, L. E. *Magnetic Resonance in Chemistry* **2003**, *41*, 843-852.

(40)   Delaglio, F.; Grzesiek, S.; Vuister, G. W.; Zhu, G.; Pfeifer, J.; Bax, A. *J. Biol. NMR* **1995**, *V6*, 277-293.

(41)   Tugarinov, V.; Kay, L. E. *J Am Chem Soc* **2006**, *128*, 7299-308.

(42)   Lundstrom, P.; Vallurupalli, P.; Religa, T. L.; Dahlquist, F. W.; Kay, L. E. *J Biomol NMR* **2007**, *38*, 79-88.

(43)   Hansen, D. F.; Vallurupalli, P.; Lundstrom, P.; Neudecker, P.; Kay, L. E. *J Am Chem Soc* **2008**, *130*, 2667-75.

(44)   Vallurupalli, P.; Hansen, D. F.; Stollar, E.; Meirovitch, E.; Kay, L. E. *Proc Natl Acad Sci U S A* **2007**, *104*, 18473-7.

(45)   Hansen, D. F.; Vallurupalli, P.; Kay, L. E. *J Am Chem Soc* **2009**, *131*, 12745-54.

(46)   Bennett, A. E.; Rienstra, C. M.; Auger, M.; Lakshmi, K. V.; Griffin, R. G. *The Journal of Chemical Physics* **1995**, *103*, 6951-6958.

(47)   Bielecki, A.; Burum, D. P. *Journal of Magnetic Resonance, Series A* **1995**, *116*, 215-220.

(48)   Metz, G.; Wu, X. L.; Smith, S. O. *Journal of Magnetic Resonance, Series A* **1994**, *110*, 219-227.

(49)   Ishii, Y. *Journal of Chemical Physics* **2001**, *114*, 8473-8483.

(50)   Bielecki, A.; Kolbert, A. C.; Levitt, M. H. *Chemical Physics Letters* **1989**, *155*, 341-346.

(51)   van Rossum, B. J.; Farster, H.; de Groot, H. J. M. *Journal of Magnetic Resonance* **1997**, *124*, 516-519.

(52)   Morris, G. A.; Freeman, R. *Journal of the American Chemical Society* **1979**, *101*, 760-762.

(53)   Meiboom, S.; Gill, D. *Rev. Sci. Instrum.* **1958**, *29*, 688-691.

(54)   Carr, H. Y.; Purcell, E. M. *Phys. Rev. J1 - PR* **1954**, *94*, 630 LP - 638.

(55)   Baldwin, A. J.; Kay, L. E. *J Biomol NMR* **2012**, *53*, 1-12.

(56)   Kay, L. E.; Torchia, D. A. *Journal of Magnetic Resonance* **1991**, *95*, 536-547.

(57)   Baldwin, A. J.; Hansen, D. F.; Vallurupalli, P.; Kay, L. E. *J Am Chem Soc* **2009**, *131*, 11939-48.

TOC